frontiers in Ecology and Evolution

TYPE Original Research
PUBLISHED 31 August 2026
DOI 10.3389/fevo.2026.1900563

Check for updates

OPEN ACCESS

EDITED BY
Kwasi Connor,
University of California, Irvine,
United States

REVIEWED BY
Yuan Mu,
Dali University, China
Sneha Suresh,
University of Massachusetts, United States

*CORRESPONDENCE
Matthew J. Powers
powersm3@oregonstate.edu

RECEIVED 04 June 2026
REVISED 03 August 2026
ACCEPTED 17 August 2026
PUBLISHED 31 August 2026

CITATION
Powers MJ and Barreto FS (2026) Genetic loci associated with natural variation in hypoxia tolerance in the copepod *Tigriopus californicus* revealed by bulked segregant analysis. *Front. Ecol. Evol.* 14:1900563. doi: 10.3389/fevo.2026.1900563

COPYRIGHT
© 2026 Powers and Barreto. This is an open-access article distributed under the terms of the Creative Commons Attribution License (CC BY). The use, distribution or reproduction in other forums is permitted, provided the original author(s) and the copyright owner(s) are credited and that the original publication in this journal is cited, in accordance with accepted academic practice. No use, distribution or reproduction is permitted which does not comply with these terms.

Genetic loci associated with natural variation in hypoxia tolerance in the copepod *Tigriopus californicus* revealed by bulked segregant analysis

Matthew J. Powers* and Felipe S. Barreto

Department of Integrative Biology, Oregon State University, Corvallis, OR, United States

The copepod *Tigriopus californicus* is among crustaceans that have recently been shown to have lost key genes encoding the master regulators of the hypoxia-inducible factor (HIF) pathway, thought to be essential for oxygen homeostasis in animals. This species inhabits supralittoral pools that impart hours of hypoxic stress daily, frequently reaching anoxia. Despite lacking the canonical HIF transcription factor, *T. californicus* exhibits one of the highest levels of tolerance to hypoxia recorded in aquatic animals. The genetic mechanisms involved in hypoxia response in taxa lacking HIF components is almost entirely unknown. We took advantage of geographic variation in tolerance in *T. californicus* to identify quantitative trait loci (QTL) using recombinant hybrids between a more tolerant California population and a less tolerant Oregon population. After quantifying individual-level tolerance in nearly 800 hybrid copepods using P_{crit}, we performed Pool-seq and bulked segregant analysis to identify QTLs. Our analysis revealed seven QTLs across five chromosomes, harboring a total of 43,648 SNPs. SNPs within these QTLs represented 721 genes enriched for stress response, sugar metabolism, neuronal signaling, and mitochondrial functions, and included genes implicated in exoskeletal and membrane modifications. Many genes in the QTLs were known in *T. californicus* to show differential expression in response to experimental hypoxic events, suggesting that some genetic variation explaining differences in P_{crit} among populations is associated with loci that are a part of acute transcriptomic responses. Most SNPs in QTLs were found in introns or within 1000 bp upstream of genes, indicating a bias toward variants with potential regulatory impacts in the QTLs. QTL genes with known transcriptional response tended to have more SNPs in these regions compared to genes that do not participate in acute responses to hypoxia. SNPs annotated as high impact, including stop lost or stop gained variants, affected over a dozen genes including an important antioxidant regulatory gene. These results provide a first glimpse at the genetic architecture underlying natural variation in hypoxia tolerance in a species lacking the key oxygen-sensing regulatory gene and highlight candidate genes of diverse biological pathways that may contribute to stress resilience in extreme environments.

KEYWORDS
exoskeleton, hypoxia inducible factor, mitochondria, oxidative stress, P_{crit}

Introduction

When aquatic organisms encounter oxygen-depleted environments, they face a serious challenge to respond via modifications to cellular function. For most species, alterations to normal biological function in response to depleted oxygen are initiated transcriptionally by key regulatory elements of the hypoxia-inducible factor (HIF) pathway, primarily the transcription factor subunit HIF-α (Gorr et al., 2010) and its dedicated repressor the O_2-dependent prolyl hydroxylase, EGLN (Kaelin, 2005). During a hypoxic event, HIF-α is no longer repressed by EGLN and it forms a dimer with HIF-β/ARNT before binding to regulatory regions called hypoxia response elements (HREs) and initiating transcription of genes involved in an array of functions, such as metabolic alterations, protein repair, or cellular detoxification (Kaluz et al., 2008). It is generally expected that any metazoan will rely on the HIF pathway for controlling physiological response to hypoxia. However, recent studies have shown that several marine organisms have lost the *HIF-α* master regulatory gene (Graham and Barreto, 2019, 2020, 2023), including several barnacle species within orders Sessilia, Pedunculata, Kentrogonida and copepod species in the orders Cyclopoida, Harpacticoida, and Siphonostomatoida. This discovery has prompted inquiry regarding the hypoxia tolerance in the absence of HIF-α. One of the members of Harpacticoida lacking *HIF-α* (as well as *EGLN*), *Tigriopus californicus*, is a marine copepod that has become an important model for understanding hypoxia tolerance in the absence of the master HIF regulatory factor (Powers et al., 2025).

An inhabitant of volatile splash pools in the supralittoral zone of the west coast of North America, *T. californicus* faces nightly challenges to extreme hypoxic events. During summer nights, photosynthetic algae that co-inhabit *T. californicus* pools deplete oxygen, even to complete anoxia for up to six continuous hours (Powers et al., 2025). This species has evolved to be extremely hypoxia tolerant, likely as a result of such selection pressure, but levels of tolerance vary geographically (Deconinck and Willett, 2022; Powers et al., 2025). The southern population from San Diego (SD), California, was recently studied for its transcriptomic response over the course of a hypoxic series mimicking the nightly hypoxia events in natural *T. californicus* pools. Despite lacking *HIF-α*, the SD copepods mounted a dynamic transcriptomic adjustment over the course of normoxia, mild hypoxia, at the species P_{crit}, during anoxia, and into early recovery, significantly adjusting expression of genes in known response pathways, such as glycolysis and antioxidant response, as well as genes involved with pathways involving exoskeletal modifications, pigment metabolism, and sugar-derivatives with protective roles during hypoxia (Powers and Barreto, 2026b). This robust regulatory response involving multiple gene networks and functions is concordant with extreme hypoxia tolerance phenotypes in *T. californicus*, but it is unknown how these genes are being regulated without HIF.

Hypoxia is considered severe at dissolved oxygen levels below 2 mg O_2 l^{-1} (Vaquer-Sunyer and Duarte, 2008). However, *T. californicus* can survive extended hypoxia exposure as long as 72 hours and even up to 24 h of complete anoxia (Powers et al., 2025). Using statistics that capture an organism's ability to regulate its respiration as oxygen decreases (such as critical oxygen tension, a.k.a. P_{crit}), we showed that *T. californicus* is among the most hypoxia-tolerant organisms studied to date. The best measurements of survival and lowest P_{crit} measurements were observed in southern populations of *T. californicus*, where among the four populations tested, two populations from California had better survival and respiratory regulation compared to two northern populations from Oregon, consistent with population-level variation in tolerance to other stressors (Healy et al., 2019). We hypothesize this phenotypic variation could be due to differences in hypoxia regimes among populations leading to local adaptation.

This variation provides an opportunity to better understand genetic components underlying cellular responses in this hypoxia-tolerant species lacking the master HIF regulator. Populations of *T. californicus* are genetically divergent across most of their genomes (Barreto et al., 2018). And while laboratory hybridization among populations produces offspring with reduced fitness, these progenies are still viable and can be propagated indefinitely. Using multigenerational hybrids from a cross between copepods from San Diego, CA (SD) and copepods from Strawberry Hill, OR (SH), we performed a bulked segregant analysis (BSA) to identify quantitative trait loci (QTL) associated with variation in tolerance to hypoxia in *T. californicus* as measured using critical oxygen tension, or P_{crit}. The advantage of identifying QTLs using this method comes from how genomes are sequenced. Bulked segregant analysis bypasses the need to sequence hundreds of individuals separately in favor of sequencing large pools of individuals grouped at opposite ends of phenotypic space (Li and Xu, 2022). Loci linked with the phenotype of interest are then identified using metrics (like G' and deltaSNP) that quantify significant deviations in parental allele frequencies between the bulks (Mansfeld and Grumet, 2018). Using this method to identify loci linked to hypoxia tolerance, we then mapped how much nucleotide variation may be associated with regulatory evolution of genes found in QTLs and examined how SNP frequencies were distributed among genes previously observed to respond via expression changes during stress. We also examined genes in QTLs for known functions related to hypoxia, oxidative stress, or newly emerging roles in tolerance for this species, such as exoskeletal modifications or alternative uses of sugar pathway intermediates (Graham and Barreto, 2019; Powers et al., 2025).

Materials and methods

Generation of recombinant hybrids

Laboratory populations of *T. californicus* collected from San Diego, CA (SD; 32.7333° N, 117.2500° W) and Strawberry Hill, OR (SH, 44.254454° N, 124.112880°W) were used to generate a hybrid population. Prior to hybridization, laboratory populations were maintained as large, outbred populations for at least two generations to remove effects of environmental carryover. Laboratory populations were maintained in 400-mL beakers at an approximate density of 300 individuals per beaker in 35 ppt artificial saltwater

(ASW) and fed a mix of live microalgae (*Isochrysis* and *Nannochloropsis*) and dried spirulina (*Arthospira platensis*).

To generate the hybrid cross, 100 unmated females from the SH population were paired with 100 males from the SD population in a petri dish and allowed to mate. Mated females from these pairings were kept in petri dishes at a density of 20–30 females per dish until they developed egg clutches. Eggs were relocated to 400-mL beakers to hatch and the F1 offspring were allowed to mate. From these matings, six hybrid lines were established using 110 mated F1 females. For each line, new generations were formed by randomly selecting 50 egg clutches from gravid females. New generations were made using this method until the 12th generation. During this period, two lines collapsed due to population crashes leaving four lines to successfully reach the 12th generation with large populations. From this point forward, hybrid lines were allowed to propagate freely and mate continuously in overlapping generations. Hybrid cultures were then propagated out into multiple beakers of continuous cultures that were admixed randomly every two weeks during partial water changes and food addition. This process produced approximately 24 beakers with healthy, outbred populations, and these were maintained for nine additional months or approximately 10 additional generations before phenotyping.

Phenotyping for bulked segregant analysis

To map genomic regions potentially associated with natural hypoxia tolerance variation, we aimed to compare allelic variation between groups, or bulks, of SHxSD hybrid copepods that differ in their level of tolerance. The power to detect genetic differences between bulks increases as trait variation increases, since this variation allows for the creation of bulks with larger differences in trait means (Magwene et al., 2011). However, even small sample sizes in a pooled sequencing approach can approximate the resolution of QTL detection with much larger sample sizes or with full sequencing of separate individuals (Shen and Messer, 2022), especially via bulked segregant analysis (Song et al., 2017; Klein et al., 2018; Zheng et al., 2018; Zhang et al., 2021). Therefore, we screened our large, outbred population of hybrids for hypoxia tolerance variation across adult individuals, with the goal of pooling the top 10% and the bottom 10% performers.

We used critical oxygen tension (P_{crit}) as the metric of hypoxia tolerance. This metric is commonly used to predict hypoxia tolerance in aquatic species (Seibel et al., 2021) and represents the point at which an organism can no longer regulate its respiratory rate independent of declining available oxygen. While P_{crit} has been criticized for being unsuitable for general comparisons across species because its measurement can be influenced by species-specific factors or experiment design, we recently showed that P_{crit} was superior to other metrics in predicting observable fitness phenotypes (survival and loss of equilibrium) at the population level in *T. californicus* (Powers et al., 2025). However, the degree to which P_{crit} could repeatedly capture interindividual variation within a population was not tested. Therefore, prior to phenotyping to create pools of individuals for BSA, we tested whether P_{crit} was repeatable when measuring the same individuals more than once. We provide details of this preliminary test in the Supplemental Methods. Briefly, we found that repeated P_{crit} measurements of the same individual copepods when analyzed using the broken-stick segmented and midpoint methods were significantly positively correlated (Supplementary Figure 1; segmented: $p < 0.001$; $\beta = 0.69$ and midpoint: $p = 0.0356$; $\beta = 0.49$), while using the broken-stick intercept was not ($p = 0.074$). The regulatory index (RI, Mueller and Seymour, 2011), another common metric, was not reproducible in the same individuals in our protocol ($p = 0.526$). Because the segmented method for calculating P_{crit} was clearly the most repeatable across the two rounds of respirometry with the same individuals, we used this method going forward when phenotyping to create our bulks.

From May 21, 2024 through April 30, 2025, we sampled individual hybrid copepods on a weekly basis from randomly selected beakers and performed respirometry to estimate their individual P_{crit}. Each week, approximately 30 females and 30 males from the culture beakers were placed in a petri dish with fresh saltwater and dried spirulina for 48 hours to acclimate all individuals to the same culture conditions. After this period, copepods were added individually to the 80-µL wells of a sterilized and calibrated microplate respirometer and sealed with strips of an impermeable adhesive film (Cytiva, USA) before being covered by a rubber gasket and weight. Dissolved oxygen in each well was monitored in a dark incubator at 18°C for up to 48 hours, and each individual was removed from its well as soon as it finished consuming oxygen and transferred to a uniquely labeled well in a 24-well plate with fresh ASW and food. Once all copepods were removed from the respirometer, individuals that depleted oxygen within the trial period and were still alive after the trial were stored at -80 °C in separate microcentrifuge tubes with a numeric ID. A total of 1,344 individuals were processed and archived in this manner (687 females and 657 males).

We calculated P_{crit} (broken-stick segmented method) for each individual using the 'respirometry' package v 2.02 (Birk, 2025) integrated into a custom looping script in R (R Core Team, 2025) we developed to analyze all individuals on a data set at once (Powers et al., 2025). We filtered out individuals in which the segmented model failed to converge when calculating P_{crit} or when the estimated P_{crit} was erroneously estimated to be less than 0 or greater than full normoxia under our testing conditions (20 kPa). This filtering left us with a distribution of 795 individuals (448 females and 347 males). Because male and female copepods are known to differ in their tolerance to hypoxia and P_{crit} variation (Powers et al., 2025), we inspected the distributions of P_{crit} values for each sex separately to identify high and low performing individuals to avoid the case where a pool could mostly contain one sex if that sex vastly outperformed the other. Indeed, we observed differences in the distribution of P_{crit} values between the sexes (Supplementary Figure 2). To create our bulks, we selected individuals with the top 10% highest and bottom 10% lowest P_{crit} measurements within each sex, comprising of 34 males per bulk and 44 females per bulk, forming a total of 78 copepods per bulk combined for DNA extraction.

Sequencing and analysis

Genomic DNA was extracted from the two pools of copepods and used to prepare whole-genome sequenced libraries. Individuals

assigned to each bulk were thawed and pooled into 1.5-ml tubes containing isolation buffer, followed by DNA extraction using a phenol:chloroform method (Sambrook and Russell, 2006). Residual RNA contaminants were eliminated through RNase A treatment incorporated into the workflow. Whole-genome DNA libraries were then generated for each pool using the Nextera DNA Library Preparation Kit (Illumina, San Diego, CA). Unique dual indices were added to each pool during a 10-cycle PCR enrichment step. Amplified libraries were size-selected on a 2.5% agarose gel, targeting fragments between 350 and 550 bp, and purified using the MinElute Gel Extraction Kit (Qiagen, Hilden, Germany). After quantification with Qubit fluorescence (Thermo Fisher, Waltham, MA), the two libraries were combined in equimolar concentrations and sequenced as 150-bp paired-end reads using an Illumina NextSeq2000 platform at the Center for Quantitative Life Sciences (Oregon State University). Following a modified version of the pipeline used by Healy and Burton (2023), reads were mapped to a hybrid pseudo-reference and SNP frequences were identified for loci known to have fixed differences between SD and SH (Han and Barreto, 2021). Details about the bioinformatic pipeline are found in the Supplementary Material. A total of 70,541,367 and 82,017,336 reads for the low P_{crit} (bottom 10%) and high P_{crit} (top 10%) bulks, respectively, were successfully mapped and filtered using this pipeline (Supplementary Tables S1–S3).

Detection of trait-associated loci

We used 'QTLseqr' package v 0.7.5.2 (Mansfeld and Grumet, 2018) for our main bulked segregant analysis. We first further filtered SNPs using the 'filterSNPs' function with the following parameters: refAlleleFreq = 0.1, minTotalDepth = 80, maxTotalDepth = 400, depthDifference = 100, minSampleDepth = 40. The resulting 781,961 SNPs were then passed through a G' analysis with a window size of 750,000 and filter threshold of 0.1. SNP coverage along the genome was checked using the 'plotQTLStats' function (Supplementary Figure 3). The sliding window size was chosen based on the ability to resolve distinct peaks and establish clear statistical significance without the risk of false positives, which increase in likelihood with smaller windows. Finally, statistically significant SNPs and QTLs were identified at a threshold of alpha = 0.01 using Benjamin-Hochberg adjusted q-values. SNPs within QTLs were annotated using snpEff v5.4a (Cingolani et al., 2012) to estimate their impact (modifier, low, moderate, or high) and specific variant type. Briefly, the impact categories modifier, low, moderate, and high are labels generated by SnpEff to help filter SNPs by the degree of their potential effects on gene transcription and translation. For example, variants in the high-impact category include nonsense mutations, frameshifts, or instances of stop-gained/lost. Examples of variants in the moderate category could critical missense mutations or splice site disruptions. Examples of low impact variants include synonymous mutations or stop-retained mutations. The modifier category is broad and can include examples of variants that change the effects of other variants, such as mutations in regulatory or upstream regions. We also compiled the gene to which each SNP was annotated and their G' value and adjusted p-value (Supplementary Table 4). In order to focus on variants in coding or probable regulatory regions, we filtered this matrix to only include SNPs that were within gene coordinates or within 1000 bp upstream of a gene, and conversely, we excluded SNPs that were annotated as downstream, greater than 1000 bp upstream, or as intergenic. We gathered additional gene-level information using GenomicRanges package v 1.6.0 in R (Supplementary Table 5).

Summarizing the SNP annotations at the gene level allowed us to statistically test differences between QTL genes grouped by predefined categories. In a recent study using the SD population, we identified 1,796 genes with a significant transcriptomic response to an exposure of worsening hypoxia followed by reoxygenation (Powers and Barreto, 2026a). The data from this study can be accessed at its public repository on GitHub (https://github.com/mjp0044/Hypoxia-time-series-gene-expression). We queried our summary of genes in the QTLs and marked genes as "DE genes" if they were also found to have significant differential expression in the transcriptomic data set. Genes that did not overlap were labeled "non-DE" genes.

Between the DE gene and non-DE genes, we tested for differences in the distribution of SNP effects and locations, and whether genes differed in the likelihood of allele frequency differences between our sequenced bulks (maximum G' statistic). To test for differences in the number of SNPs by impact (modifier, low, moderate, or high) or the number of SNPs per genomic region (upstream, in exon, in intron, or in the gene in general), we fit a quasipoisson general linear model (glm) to model counts and to control for overdispersion. For models that examined differences in SNP counts in exons and introns or SNP counts for each of the impact categories, we included a gene length as a fixed-effect offset to model the SNP counts as a rate of occurrence normalized by gene length. For models of upstream SNP counts, we include the number of SNPs in the gene per kb as a fixed effect. We also modeled differences in gene length between the groups of genes by fitting a Gamma glm with log link function to model right-skewed data like length measurements. Diagnostics were checked for each model (residual vs fitted, Q-Q of residuals, scale-location, and residuals vs leverage) to ensure statistical assumptions were not violated.

Because the SD population was previously shown to have a greater tolerance of hypoxia based on P_{crit} and survival (Powers et al., 2025), we created a secondary grouping of genes based on the frequency of parental alleles in the QTLs. For each SNP in the QTLs, we calculated the frequency of the SD allele in the low or high P_{crit} bulks. We then plotted these frequencies and examined whether the SD allele had a higher or lower frequency in the low P_{crit} bulk compared to the high P_{crit} bulk. We labeled as "SD-biased" the QTLs in which the SD allele frequency was higher in the low P_{crit} (higher tolerance) bulk, and as "SH-biased" the QTLs in which the SH allele was higher. We then compared these two sets of genes by their SNP locations and impacts, as described above for the DE *versus* non-DE genes comparisons.

Tests for functional enrichment and protein evolutionary rates of genes in QTLs

We performed tests for functional enrichment of gene ontology (GO) using the R package topGO v2.60.1 (Alexa and Rahnenfuhrer, 2025) and semantically reduced GO term complexity to umbrella

categories using rrvgo v1.20.0 (Sayols, 2023), focusing on the Biological Process (BP) ontology. This was examined at three levels. We first assessed functional enrichment of genes in QTLs overall, relative to the genome. Secondly, we examined GO terms within DE and within non-DE QTL gene groups to assess differences in function between QTL genes with and without known transcriptional response to hypoxia. Finally, the test was performed for the groups of genes in SD-biased and SH-biased QTLs to assess whether different biological processes were contributed by the two populations.

To connect our findings to those of past studies in this system, we examined how certain cellular functions of interest were represented among genes in QTLs. We obtained sets of genes we previously curated (Powers and Barreto, 2026b), which include genes whose products localize to the mitochondria (610 genes), antioxidant genes (44 genes), genes with known roles in exoskeletal or cuticle modification pathways (223 genes), known and putative pigment genes (22), and genes in sugar metabolism pathways (196 genes including glycolysis, pyruvate, TCA, pentose-phosphate, fructose-mannose, and starch-sucrose pathways). These groups represent broad functional categories with known or emerging roles in hypoxia or general stress response (Powers and Barreto, 2026b). These lists were curated previously by mining the Kyoto Encyclopedia of Genes and Genomes (KEGG) using *T. californicus* proteome accessions. The full lists of these gene groups can be found in a public repository at GitHub (https://github.com/mjp0044/Hypoxia-time-series-gene-expression).

We quantified protein evolutionary rates by estimating the ratio of rates of nonsynonymous and synonymous substitutions (d_N/d_S). This value was calculated for all QTL genes as well as for an equal number of randomly chosen genes outside of QTLs. Coding sequences from the SD and SH references were aligned using codon-aware in PRANK (Loöytynoja and Goldman, 2008) and alignments were polished with Gblocks version 0.91b (Castresana, 2000) (parameters: -t=c -b1 = 2 -b2 = 2 -b3 = 6 -b4 = 12). We then used the maximum likelihood method YN00 (Yang and Nielsen, 2000) within PAML v4.7 (Yang, 2007) to estimate gene-wide d_N, d_S, and d_N/d_S. We modeled the difference in d_N/d_S between the QTL genes and randomly selected genes using a Gamma glm with log link function. Secondarily, we also inspected whether DE and non-DE genes differed in d_N/d_S as well as genes located on the SD-biased vs SH-biased QTLs.

Results

Distribution of QTL associated with P_{crit}

G' prime analysis identified seven significant QTLs across 5 chromosomes, harboring a total of 43,648 SNPs with statistically significant differences in allele frequency between bulks (Figure 1; Table 1). Over 93% of these SNPs were annotated by SnpEff as 'modifier' variants, which are located on non-coding regions with unclear impact (Table 2). This category includes variants in introns, upstream/downstream, in intergenic regions, in 5'/3' UTRs, or that were non-coding transcript variants (Table 3). The remaining ~7% of SNPs were annotated as 'low', moderate', or 'high impact'. The 28 variants with high impact (these included splice site disruption and stop-gained/lost) affected 26 different genes. With regards to position, most SNPs were located upstream, downstream, or in intergenic regions (Tables 2, 3), but over 25% were annotated as exonic (n = 5,124) or intronic (n = 15,569). A total of 751 different protein-coding genes harbored at least one SNP within QTL regions. We filtered this list down to 721 genes by removing any SNPs farther than 1000bp upstream, SNPs downstream, or intergenic SNPs (Supplementary Table 5). We used this list of 721 genes for further downstream analyses.

Tests for GO term overrepresentation among the 721 genes in QTLs using topGO revealed a total of 133 significant terms. Semantic reduction of these terms resulted in 40 significant BP umbrella terms (Supplementary Figure 4). These included terms relevant to hypoxia response such as regulation of respiratory burst (4 subterms), carbohydrate derivative metabolic process (6 subterms), cellular response to glucose stimulus (4 subterms), regulation of nitric oxide metabolic process (2 subterms), and protein localization to mitochondrion (1 subterm). The top 10 genes ranked by maximum G' and minimum q-value within QTLs were populated with genes enriched for GO terms related to response to stress, development, the cell cycle, muscle activity, and regulation of biological processes (Supplementary Figure 5). Several of these genes have putative roles affecting energy metabolism, responses to oxidative stress, or glycolytic activity (Supplementary Table 6).

The 721 genes in the QTLs showed no significant difference in d_N/d_S values compared to randomly selected background genes from the rest of the genome (Supplementary Figure 6). Among the

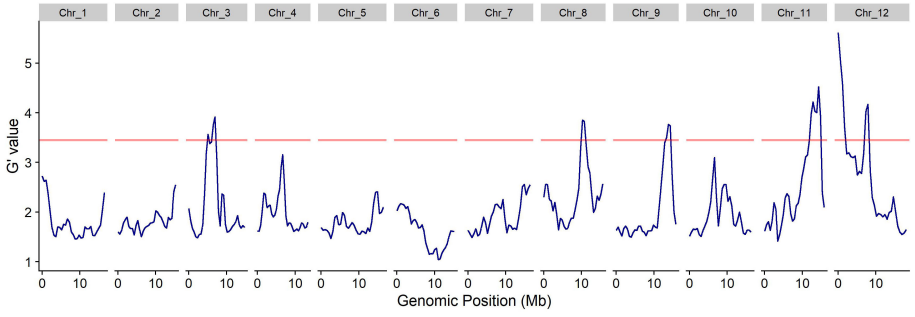

FIGURE 1
QTL analysis of P_{crit} using G'. Seven QTLs are significantly associated with hypoxia tolerance measured by critical oxygen tension. Significance (horizontal red line) was established at a threshold of alpha = 0.01 using Benjamin-Hochberg adjusted q-values from the QTLseqr package in R.

TABLE 1 Summary of QTL locations, the number of SNPs, maximum and mean G′, and mean Benjamin-Hochberg adjusted *p*-value per QTL (*q*-value).

QTL	Chrom	Start	End	nSNPs	Max G′	Mean G′	Mean *q*-value
1	11	11,856,574	14,954,097	15,510	4.52	4.05	0.002
2	12	23,727	1,979,042	6,601	5.62	4.49	0.002
3	12	6,962,023	8,230,838	3,560	4.17	3.87	0.003
4	3	4,952,701	5,379,803	2,220	3.57	3.50	0.009
5	3	6,067,420	7,207,059	4,718	3.92	3.68	0.005
6	8	9,916,999	11,136,297	6,534	3.85	3.73	0.004
7	9	13,084,602	14,453,510	4,505	3.77	3.63	0.004

26 genes with annotated SNPs that fell into the high impact category (see Table 1 for specific variant types), a specific gene stands out as potentially relevant to the control of O_2 diffusion across *T. californicus* membranes. The gene *mesh* encodes a critical protein for organizing septate junctions between cells in endothelial tissues which affect the flow of ions and solutes across tissues (Izumi et al., 2012). At total of 81 SNPs annotated to *mesh*, with nearly all of these (n = 79) occurring inside the gene. Among these, 1 was annotated as moderate impact (a missense mutation at aa position 181 of 1063), and 1 was high impact (a splice acceptor variant). The splice acceptor variant was located in the 3' UTR and likely has no impact on the coding sequence but could potentially affect mRNA processing.

TABLE 2 Distribution of effects and locations of 43,658 SNPs within QTLs, estimated by SnpEff.

Effects by impact		
Type	Count	Percent
High	28	0.04%
Moderate	1,587	1.98%
Low	3,911	4.89%
Modifier	74,495	93.09%
Effects by functional class		
Type	Count	Percent
Missense	1,595	30.91%
Nonsense	9	0.17%
Silent	3,556	68.92%
Annotations by region		
Type	Count	Percent
Downstream	17,255	21.53%
Exon	5,124	6.40%
Intergenic	21,834	27.29%
Intron	15,569	19.46%
Splice site acceptor	8	0.01%
Splice site donor	3	0.004%
Splice site region	356	0.45%
Upstream	18,121	22.65%
3' UTR	857	1.07%
5' UTR	924	1.16%

Association with transcriptomic response

We examined how the 1,796 genes with a transcriptomic response from our previous study (Powers and Barreto, 2026b) were represented among those within QTLs. We found that 101 of the 721 QTL genes were found to respond transcriptionally to hypoxia (DE genes), with the remaining 620 not observed to have significant expression response (non-DE genes). This overlap does not represent a significant enrichment among QTL genes (Fisher's exact; OR = 1.18, $p = 0.129$). To characterize possible differences in SNP content between DE genes and non-DE genes, we examined other metrics. First, we found that DE genes and non-DE genes did not differ in maximum G' values or d_N/d_S (Figures 2A, B). With respect to SNP location, there was also no significant difference between the two sets of genes in the frequency of SNPs upstream, in exons, nor any difference in gene length (Figure 2C). However, DE genes had significantly more SNPs per kb of gene, and this difference appears to be largely driven by the number of SNPs located in introns (Figure 2C). Concordantly, the DE genes also had significantly more SNPs annotated under the 'modifier' category compared to non-DE genes (Supplementary Figure 7).

DE genes were enriched with different GO terms compared to non-DE genes (Supplementary Figure 8). Umbrella biological processes enriched in the DE genes included negative regulation of transporter activity (4 terms), adaptive immune response (3 terms, including response to oxygen-containing compound), plasma membrane organization (3 terms), negative regulation of ATP-dependent activity, and endocytic recycling (3 terms), and regulation of cell conduction (2 terms) and muscle cell action potential (1 term). Non-DE genes were enriched for GO terms related to separate regulatory processes (Supplementary Figure 8). Some of these were negative regulation of epithelium morphogenesis (4 terms), regulation of calcium ion sequestration (3 terms), regulation of muscle cell proliferation (3 terms), negative regulation of nervous system development (3 terms), positive regulation of D-glucose transmembrane transport (3 terms), regulation of nitric oxide metabolism (2 terms), and positive regulation of transcription by RNA polymerase II (2 terms). Some other notable enriched GO terms in the non-DE genes include response to osmotic stress (4 terms), cellular response to glucose stimulus (3 terms), and protein localization to the mitochondrion (1 term).

TABLE 3 Variant types organized by SnpEff-annotated impact categories in the SNP dataset.

Annotation	Modifier	Low	Moderate	High
3' UTR variant	857	–	–	–
5' UTR variant	889	–	–	–
Upstream gene variant	4,479	–	–	–
Intron variant	15,569	–	–	–
Stop retained variant	–	1	–	–
Splice region variant & Stop retained variant	–	3	–	–
Splice region variant	–	12	–	–
Splice region variant & synonymous variant	–	33	–	–
5' UTR premature start codon gain variant	–	35	–	–
Splice region variant & Intron variant	–	308	–	–
Synonymous variant	–	3,519	–	–
Missense variant & Splice region variant	–	–	29	–
Missense variant	–	–	1,558	–
Stop gained & Splice region variant	–	–	–	1
Stop lost & splice region variant	–	–	–	2
Splice donor variant & intron variant	–	–	–	3
Start lost	–	–	–	6
Stop gained	–	–	–	8
Splice acceptor variant & splice region variant	–	–	–	8

Parental allele frequencies associated with low P_{crit}

We examined each QTL to determine which parental allele was more frequently associated with low P_{crit}. We found that the five QTLs on chromosomes 3, 11, and 12 were defined by higher frequency of SD alleles in the bulk with low P_{crit} (higher tolerance) than with high P_{crit} (lower tolerance). Conversely, the QTLs on chromosomes 8 and 9 had a greater frequency of SH alleles in the low P_{crit} than high P_{crit} bulk (Figure 3A). These biases in the QTLs represent statistically significant (Chi-squared text, $p < 0.0001$) departures from the background frequency of the SD allele on the rest of the chromosome (Supplementary Table 7), with the QTLs on chromosomes 3, 11, and 12 having a higher SD allele frequency than background SNPs on the rest of those chromosomes (Supplementary Table 7). The QTLs on chromosomes 8 and 9 had departures with the opposite pattern (Supplementary Table 7).

At the gene level, a greater proportion of genes present across all the QTLs were biased toward the SD allele in the low P_{crit} bulk (69.07%, 498 of 721 genes). Genes in these SD-biased QTLs had significantly more SNPs per kb of gene length than SH-biased QTLs (Supplementary Figure 9A). This was driven by a significantly higher number of SNPs found in the introns in genes in the SD-biased QTLs. The two sets of genes did not differ in the number of SNPs in exons or the number of SNPs 1000 bp upstream. Genes in SD-biased QTLs had significantly higher G' values compared to genes on SH-biased QTLs (Supplementary Figure 9B). Genes in SD-biased QTLs were more likely to have higher d_N/d_S values than genes on SH-biased QTLs, though this effect size was modest (Supplementary Figure 9C). We found no significant differences in the number of SNPs annotated to the modifier, low, moderate, or high impact categories as defined by SnpEff (Supplementary Figure 9D).

Semantic reduction of individual GO terms to parent-term groupings revealed that genes found in SD-biased and SH-biased genes QTLs were involved largely with different functions. SD-biased QTLs were enriched with genes involved in biological processes related to carbohydrate and lipid metabolic processes, plasma membrane organization, cellular response to hormone stimulus, regulation of nervous system development, regulation of transcription, regulation of responses to external stimuli, and spermatogenesis (Figure 3B). SH-biased QTLs were enriched with terms involving energy derivation by oxidation reactions, supramolecular fiber organization, protein localization to cell membranes, cell surface receptor signaling, tRNA processing, and muscle development (Figure 3B).

Functions related to hypoxia responses in QTLs

Five genes from the list of genes involved in glycolysis, TCA, pentose-phosphate, and starch-sucrose pathways were found in QTLs (Supplementary Table 8). Among these were a *Tret1* gene, which encodes a transporter of the sugar trehalose that has known protective roles against hypoxic stress in invertebrates (Chen et al., 2002; Zhang et al., 2025). SNPs annotated to this gene were mostly upstream or in introns (n = 12 and 25, respectively) and all exonic variants were predicted to have no effect on the coding sequence. Additionally, two genes with known transcriptional responses to hypoxia in *T. californicus* were among these five genes; these were annotated to *Shpk*, which encodes a sedoheptulokinase in the

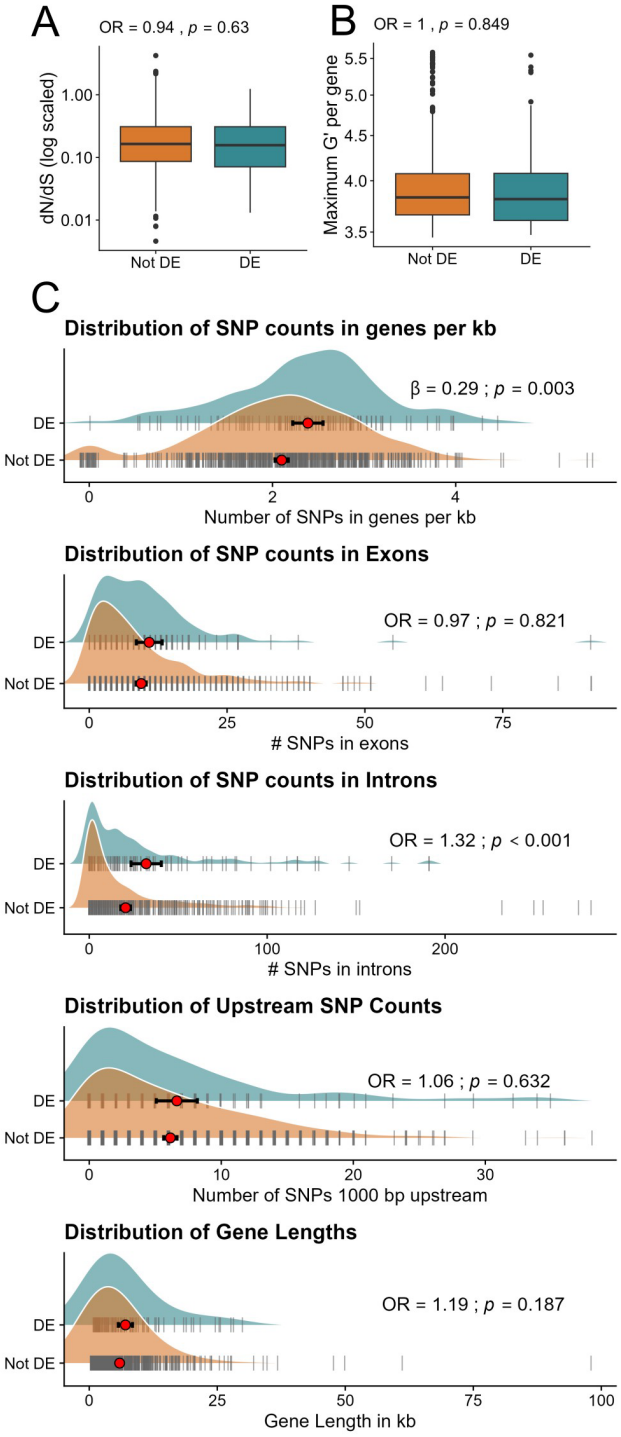

FIGURE 2
Comparison of SNP features among QTL genes with known differential expression (DE) during hypoxia. Boxplots show median and IQR of **(A)** d_N/d_S and **(B)** maximum G'. Odds ratios (OR) are from a gamma glm and are interpreted with the DE group as the reference. **(C)** Ridgeline plots of the density of SNPs in various regions in or upstream of genes in the QTLs as well as gene length. The mean and confidence interval for each distribution is marked with the red dot and black bars. Grey dashes mark the individual SNP counts per gene. Odds ratios are from a quaispoisson glm and are interpreted with respect to DE genes as the reference group. The β is from a linear model.

pentose phosphate pathway, and *Akr1a1*, which encodes an alcohol dehydrogenase in the pyruvate pathway. There were 39 SNPs annotated to *Shpk* and 3 of these were missense variants while *Akr1a1* had 43 total SNPs with 1 being a missense variant.

Among our functional groups of interest, mitochondrial genes had the greatest representation in the QTLs, with 23 genes (Supplementary Table 8). This list included several genes involved in interactions between the mitochondrial and nuclear (mitonuclear) genomes; 2 genes encoding mt-aminoacyl tRNA synthetases (mt-ARS, *Hars* and *WARS2*, each with 1 missense variant), 2 encoding mitochondrial ribosomal proteins (mt-RP, *mRpL10* and *mRpS26*, with 2 and 1 missense variants, respectively), 1 encoding a translation

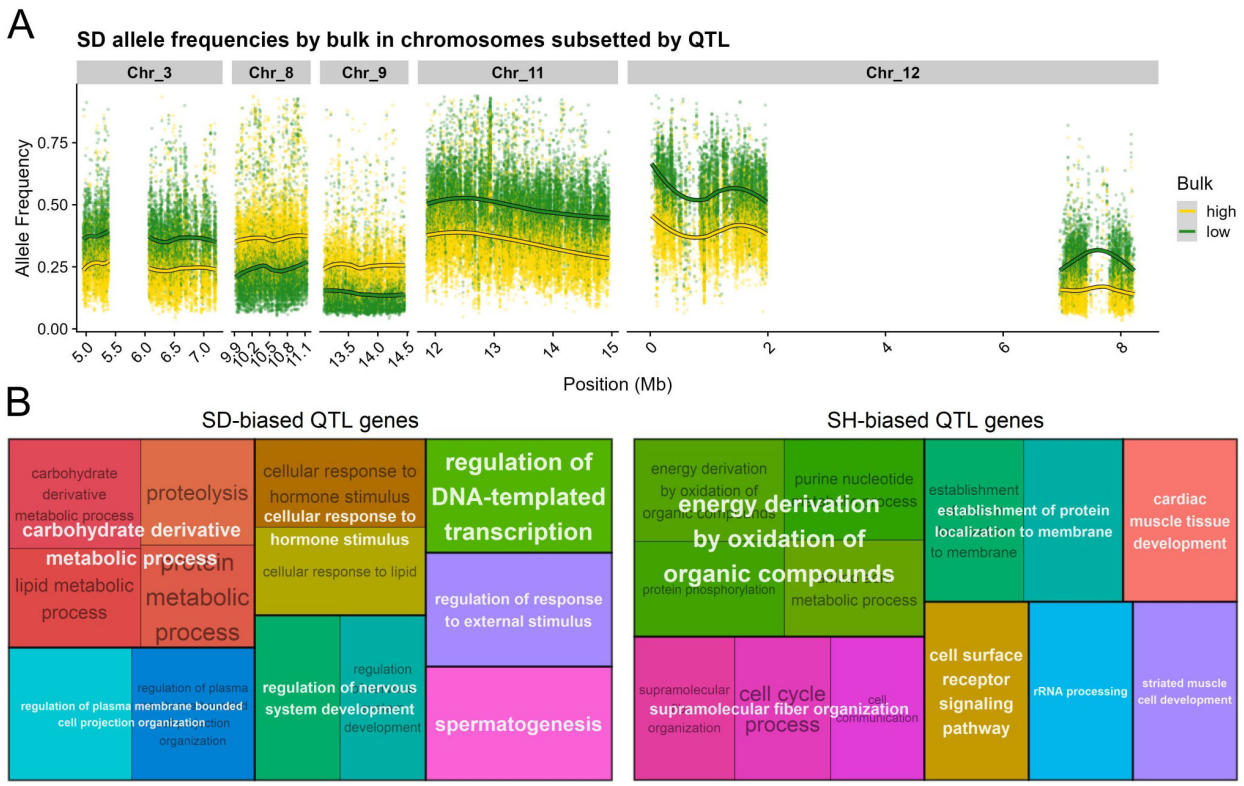

FIGURE 3
Pattern of population-of-origin of SNPs in QTLs. **(A)** Frequency of the SD allele in SNPs in the high P_{crit} (lower tolerance, yellow) and low P_{crit} (higher tolerance, green) bulks. The line shows the smoothed conditional mean among SNPs along each local chromosomal region where the QTL was detected. **(B)** Treemaps of semantic reduction of enriched Gene Ontology terms for genes in the SD-biased QTLs and SH-biased QTLs. Where boxes are blank, the child-term became the umbrella term for the entire group.

factor (*Mtif2*, with 3 missense variants), and 1 encoding a subunit of ATP synthase (OXPHOS complex V, *ATPsynCf6*). Among the 17 other genes encoding mitochondria-targeted products in QTLs, we found *BCKDHA*, which is required to produce Acyl-CoA to supply the TCA cycle, and *Trap1*, which encodes a mitochondria heat shock protein.

The lone OXPHOS gene present in the QTLs encodes the protein ATPsynCf6, or ATP Synthase Coupling Factor 6, which is a subunit of ATP synthase (complex V) in mitochondrial oxidative phosphorylation. Its primary role is to connect the head of ATP synthase to the membrane rotor, enabling ATP synthesis from proton motive force (Walker and Dickson, 2006). All SNPs annotated to *ATPsynCf6* were either in introns or upstream (Figures 4A, B). This gene is flanked in the QTL on chromosome 11 by other genes of potentially relevant function to hypoxia. For example, the gene *slc44a2* encodes a choline transport family protein that localizes specifically to the mitochondrial membrane and allows for choline transport into the mitochondria that is crucial to maintain mitochondrial energetics (Kenny et al., 2025). SNPs annotated to *slc44a2* had the highest ΔSNP values in this region (Figure 4A) and included many in exons (n = 48, compared to n = 16 in introns and n = 10 upstream), of which 18 were missense variants. Four other choline-related genes were found across the QTLs, implicating a possible involvement of choline-acetylcholine flux during hypoxia in *T. californicus* (*slc44a1*, *ACHE1*, *ChT*, and *Cha*). The gene *Cha* had the fourth highest G' prime values in QTL 3 located on chromosome 12 (Supplementary Table 6).

We found one gene encoding an antioxidant enzyme in the QTLs, *GSTT1*, which encodes a transferase in the glutathione antioxidant system (Supplementary Table 8). However, we did observe genes that help control antioxidant activity with other functions. For example, the gene *Cyp6a14* was among the 26 genes with high impact SNPs, found in the SD-biased QTL on chromosome 11 (Figures 4C, D). This gene encodes an epoxidase with known regulatory roles of antioxidant responses during oxidative stress in invertebrates (Wang et al., 2026). Only 10 SNPs were annotated to this gene, but one of these is predicted to be a stop-lost variant leading to the addition of two additional terminal amino acids in the SH allele (Figure 4E). Only one putative pigment gene was found in QTLs, *CD63*, known to be involved in melanosome formation for pigmentation (van Niel et al., 2011). There were four missense variants annotated to this gene (Supplementary Table 5).

Previous studies have suggested a possible role of exoskeletal, cuticle, and or epithelium modification in hypoxia tolerance in *T. californicus*, possibly by affecting oxygen flow across tissues (Graham and Barreto, 2019; Powers and Barreto, 2026b). Among genes with known involvement in exoskeletal modification, 11 were found in QTLs (Supplementary Table 8). These included genes which encode four pro-resilins, a chitinase, two proteins that work in the chitin synthesis pathway, a trehalose transporter, and the

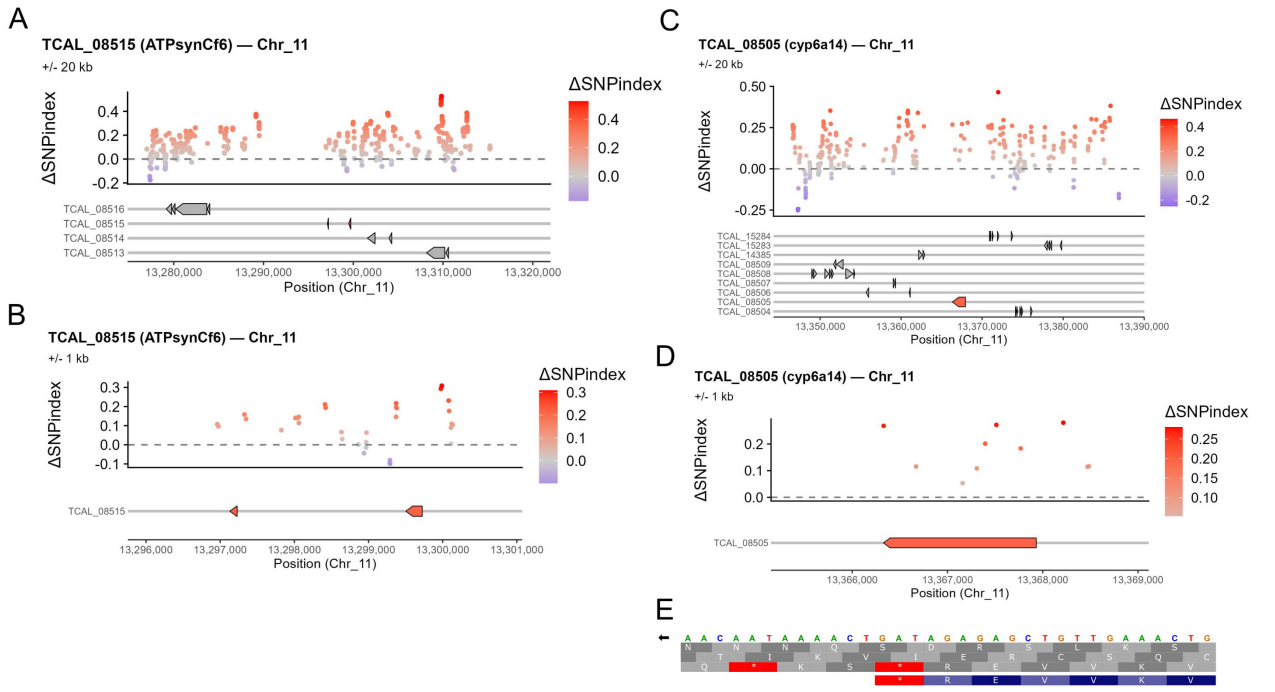

FIGURE 4
Gene tracks of *ATPsynCf6* and *Cyp6a14*. **(A, C)** Region of 40 kb window and **(B, D)** zoom window centered at the focus gene. Plotted above gene tracks are the delta SNP index values of SNPs along the track, where positive values indicate the SD allele was more common in the low P_{crit} bulk. Arrows on gene track represent exons. **(E)** Amino acid translation for *Cyp6a14* of the end of the gene, with stop codons marked in red. This gene has a stop-lost variant in which the SH allele gained two codons before the next stop. Gene ID legend: TCAL-08516 = *unc-22*, TCAL-08515 = *ATPsynCf6*, TCAL_08514 = *LAC*, and TCAL_08513 = *slc44a2*, TCAL_15284 = *HEB2*, TCAL_08505 = *Cyp6a14*, and TCAL_08504 = *HEB1*. TCAL_15283, TCAL_14385, TCAL_08509, TCAL_08507, and TCAL_08506 are proteins of unknown function.

primary enzyme responsible for cuticle sclerotization and tanning in arthropods, *Laccase2* (*lcc2*), located on chromosome 3. *Lcc2* was also among DE genes (Supplementary Table 8). While many SNPs annotated to *Lcc2* were upstream or located in introns (Supplementary Figure 10), there were also 3 exonic SNPs annotated as missense variants. *Lcc2*, along with 8 of the other cuticle/exoskeleton modifying genes, were in SD-biased QTLs. Two other genes in the chitin synthesis pathway, *GALK1* and *GFPT1*, were among SH-biased QTLs, located on chromosomes 9 and 8, respectively. Both *GALK1* and *GFPT1* had 2 missense variants. The expression of both genes was previously shown to significantly change during hypoxia exposure (Supplementary Table 8).

Discussion

We previously demonstrated that the intertidal copepod *Tigriopus californicus* is extremely tolerant to hypoxia and that this species can mount a rapid and robust transcriptomic response during hypoxic events (Powers et al., 2025; Powers and Barreto, 2026b). Using multigenerational hybrids between two phenotypically divergent populations of *T. californicus* copepods, we identified genomic loci associated with hypoxia tolerance as measured by critical oxygen tension (P_{crit}). These seven loci spread across five chromosomes include genes involved in a variety of processes involving cell signaling, regulatory processes, and stress response pathways, including cholinergic flux, cuticle remodeling, and mitochondrial function. It appears that the canonical hypoxia response regulator, *HIF-α*, is not required to explain variation in P_{crit} among populations. Widespread compensatory evolution across the genome may be sufficient to produce variation in a hypoxia-resistant phenotype in *T. californicus* without this key gene used by most other aerobic taxa. Our findings add new information about the cellular functional network that may have evolved to accommodate loss of ancestral HIF pathway regulators.

Previous work has shown that copepods from more southern populations (like SD), exhibit a greater tolerance to hypoxia compared to those from northern latitudes (Powers et al., 2025). The two parental populations in our study were chosen because they showed divergent levels of P_{crit} profiles, so it is expected and reassuring that the majority of QTLs, and those with highest strength, were defined by a higher SD allele frequency in the low P_{crit} bulk. This finding is strengthened by the fact that the genome-wide background frequency was biased towards SH alleles (Supplementary Table 7). This starting SH-biased genome is likely a consequence of long-term selection for matching between nuclear and mitochondrial background that is known in this system (Burton et al., 2006; Barreto et al., 2018) and was expected to occur in this cross (SH mtDNA and recombinant SHxSD nuclear genome) after many generations (Pereira et al., 2021). Regions associated with the SD-biased QTLs likely explain the majority of the P_{crit} variation among natural populations. Interestingly, by using late-generation hybrids, our analyses also revealed genomic

regions that harbor advantageous alleles from the SH populations. These were the two QTLs on chromosomes 8 and 9, which had a drastic decrease in the SD allele frequency in the low P_{crit} bulk. This observation indicates that our QTLs captured loci that have independently evolved tolerance-associated variants in the SH population that are not a major part of the response in SD populations. Hybrids of SHxSD with the lowest P_{crit} hence enjoy a full complement of high-tolerance alleles from both genomes. It is reasonable to expect that a complex phenotype like hypoxia tolerance is shaped by selection acting on multiple genomic targets among populations. The single phenotype we measured, P_{crit}, while a standard and widely used metric to approximate hypoxia tolerance, has been criticized for broadly capturing the effects of many different mitochondrial, cellular, and metabolic processes (Mueller and Seymour, 2011; Farrell et al., 2021). Therefore, we expect the QTLs to affect different sub-processes captured by P_{crit}. Our analysis revealed tolerance-associated variants from both parental backgrounds, and this is consistent with polygenic local adaptation (Anderson et al., 2013) that influences variation in P_{crit} among allopatric populations with no gene flow.

Our analyses also found evidence that differences in P_{crit} are due in large part by variation in regulatory regions, rather than coding sequence variation. This is supported by the observations that SNPs in introns, when corrected for differences in gene length, drives the difference between DE and non-DE genes (Figure 2), and that DE genes had significantly more SNPs annotated to the modifier category (which includes variants that cause regulatory changes) than non-DE genes (Supplementary Figure 7). Moreover, d_N/d_S across all QTL genes was not higher than in background genes (Supplementary Figure 6). This result argues against relaxed selection being the sole driver of differences in hypoxia tolerance captured by the QTLs and could suggest a greater role for regulatory divergence explaining variation in P_{crit}. Since genes in SD-biased QTLs had more intronic SNPs than SH-biased ones, effects of gene regulation are likely more important in the hypoxia response of SD populations. We do not have the power to annotate specific intronic SNPs regarding the direct impact on gene regulation, but we argue that our finding here suggests that genetic differences between SD and SH in genes with high proportion of intronic SNPs is likely associated with evolution of expression levels as a mechanism of hypoxia tolerance. This result, in combination with GO enrichment for regulatory processes (Figure 3; Supplementary Figures S4, S5, S8), suggests that variation in P_{crit} among populations of *T. californicus* may be partially explained by differences in gene expression.

It is important to caveat that QTL genes were detected here using SHxSD hybrids while the transcriptional response to hypoxia were identified using SD copepods (by Powers and Barreto, 2026b). Therefore, we cannot be certain to what degree the overlap between the two sets of genes represent variation of evolved regulatory mechanisms that would affect the hypoxia response of gene expression among populations. Future research should aim to compare differences in the hypoxia responsiveness of gene expression across individuals varying in SNP alleles we found to be in putative regulatory regions associated with P_{crit} QTLs.

Among the manually curated lists of genes organized by function, the largest group represented in the QTLs belonged to genes whose products function in the mitochondria. This is consistent with mitochondria being an important cellular target for adaptation to hypoxia stress due to its central role in oxidative phosphorylation and ROS generation. Across all QTLs, we detected enrichment of genes involved in the protein localization to the mitochondria (GO:0070585, 9 genes total in the QTLs). We had previously found that genes whose expression increased during hypoxia but decreased during recovery were enriched not for mitochondrial protein localization itself, but the positive regulation of this process (GO:1903955, Powers and Barreto, 2026b). This indicates that baseline protein transport to the mitochondria may influence variation in P_{crit} among populations, while the transcriptional adjustment of this process is key for acute response to hypoxia. It is possible that the involvement of mitochondrial variants in the QTLs could be partially explained by selection on mitonuclear compatibility to enable proper mitochondrial function through coordination between the maternally inherited SH mitochondrial DNA and the nuclear genome. However, we do not think this is likely. Previous research has shown that maladaptive mitonuclear genotypes in *T. californicus* can be removed from hybrid populations over just nine generations (Pereira et al., 2021). In comparison, the hybrids we sequenced were more than 22 generations old. Moreover, several genes which encode products targeted toward mitochondrial function were present in the SD-biased QTLs (Supplementary Table 6) and ~69% of all candidate genes were present in SD-biased QTLs, indicating that selection for mitonuclear compatibility alone does not explain the presence of mitochondrial genes in the QTLs.

A potentially important gene from the mitochondrial list found in the QTLs is *Oxa1l*. This gene encodes a key mitochondrial inner membrane protein that controls integration of several other proteins into the inner mitochondrial membrane, including during the biogenesis and assembly of complex I, IV, and ATP synthase (Stiburek et al., 2007). In our study, *Oxa1l* was found within an SH-biased QTL on chromosome 8 and is surrounded by six other genes within a 20-kb window (Supplementary Figure 11). Among these are three other putative mitochondria-targeted genes: *Trap1*, which encodes a heat shock protein that modulates the balance between oxidative phosphorylation and glycolysis (Yoshida et al., 2013), *TDH*, which encodes a threonine dehydrogenase necessary for mitochondrial biogenesis (Li et al., 2024), and a paralog of *Oxa1l* (hereafter *Oxa1l.2*). Both *Oxa1l* copies harbored seven missense SNPs in our dataset but differed in that *Oxa1l* had 16 SNPs located upstream, while *Oxa1l.2* had none. Concordantly, *Oxa1l* is among DE genes while *Oxa1l.2* is not (Supplementary Tables S5, S8). Assuming these paralogs have similar insertase functions in *T. californicus*, this could represent a scenario in which evolution at the genomic level influences separate components of protein integration in the mitochondrial membrane. Since these paralogs are very close together, however, we cannot speculate if either is more important in hypoxia tolerance variation in *T. californicus*.

Beyond the import and export of proteins, the mitochondria are also tightly linked to cholinergic flux. Choline is a dietary-derived

ammonium cation. This compound is the required substrate to produce the neurotransmitter acetylcholine (ACh) which is widely known for its roles in the central and peripheral nervous systems. However, cholinergic flux influences mitochondrial function and apoptosis during oxidative stress through receptors located on or signaling to the mitochondria (Lykhmus et al., 2023; Sonobe et al., 2025). The genes *Cha* and *ACHE1* encode enzymes that control cholinergic tone, where Cha facilitates the conversion of choline to the neurotransmitter acetylcholine and ACHE1 hydrolyzes acetylcholine back to choline. Both genes contained missense variants (Supplementary Table 5) and showed decreased expression during anoxia but increased expression during recovery (Powers and Barreto, 2026b). Moreover, *Cha* was among the genes with the most significant G' values in the QTLs (Supplementary Table 6). Previous studies have indicated Cha may reduce metabolic demand during hypoxia and facilitate a shift to glycolytic energy production through a mechanism of non-neuronal induction of *HIF-α* (Kakinuma et al., 2013). However, without *HIF-α* in the *T. californicus* genome as a downstream target, it will be interesting to examine the possible role of this protein in hypoxia response.

Regardless of acute transcriptomic responses to hypoxia involving these elements of the choline pathway, the presence of *Cha*, *ACHE1* and choline transporters *ChT*, *slc44a2*, and *slc44a1* in the QTLs suggests there is at least some constitutive genetic variation in the choline pathway associated with P_{crit} variation. This could imply different baseline cholinergic tone and mitochondrial choline supply contributing to differences in P_{crit} among populations. The genes *Cha*, *ChT*, and *slc44a2* were found in SD-biased QTLs, while *ACHE1* and *slc44a1* were found in SH-biased QTLs. The opposing biases across these five genes could reflect that SD and SH populations have evolved different solutions to optimizing baseline choline-acetylcholine flux during hypoxia.

Among the top 10 significant genes per QTL were several genes that have been shown in other systems to be associated with cellular response to hypoxia, including *Pld1*, *CycA*, *Cha*, *Mpo*, *Col1a2*, and *Mlc2* (Supplementary Table 6). Because the usual hypoxia response typically requires modulation of glycolytic pathways, it is also notable that several genes with known involvement with glycolysis were among the top significant genes (Supplementary Table 6). These include *C2cd5*, which stabilizes glycolytic activity and helps control mitochondrial trafficking (Gavini et al., 2022; Yang et al., 2026) and *Kdm8*, shown to upregulate glycolytic genes and promote glycolysis during hypoxia (Wang et al., 2019).

More broadly, several of the top genes are associated with responses to oxidative stress or control of antioxidant activity (Supplementary Table 6). Interesting cases from this group include *CPSF4*, which encodes a factor shown to affect transcription during oxidative stress (Liu and Manley, 2024), *TMLHE*, which may help limit ROS generation during oxidative stress through its effects on carnitine biosynthesis (Liepinsh et al., 2021), and *SP4*, which regulates all 13 subunits of mitochondrial cytochrome *c* oxidase and is hypothesized to upregulate antioxidant activity in neural cells (Mao et al., 2009; Nair et al., 2016). Only one QTL gene, *GSTT1*, encodes a member of glutathione antioxidant system, despite this system being highly responsive at the transcriptional level (Powers and Barreto, 2026b). However, a purported key regulator of the antioxidant response in invertebrates, *Cyp6a14*, was not only in QTLs but also had a stop-lost variant annotated to it. This mutation results in a difference of two terminal codons between SD and SH (Figure 4E). We cannot be certain this would result in a functional change, but we predict buffering membranes and proteins against the damaging effects of ROS to be critical for regulating respiration in the face of declining oxygen.

Besides the effects of antioxidants, it is also possible to contain the spread of ROS to buffer sensitive tissues by controlling diffusion across tissues. The gene *mesh* may be a potential candidate affecting the spread of ROS or the flow of oxygen in endothelial membranes, particularly protecting cells in the gut (Izumi et al., 2012) as the protein it encodes affects smooth septate junctions. These junctions can affect diffusion across tracheal cells (Paul et al., 2003; Wu and Beitel, 2004), but future research is required to test whether their roles in forming cellular diffusion barriers could affect hypoxia tolerance. This idea is speculative but is worth considering in a system like *T. californicus*, which lacks a circulatory system, respiratory organs, or gills and, instead, relies on passive oxygen diffusion to oxygenate its tissues.

The reliance on oxygen diffusion across the cuticle and exoskeleton for mitochondrial respiration in *T. californicus* has prompted consideration that modifications to the cuticle membranes or chitin-based exoskeleton may be key for this species to survive hypoxic events (Graham and Barreto, 2019; Powers and Barreto, 2026b). Our QTLs included genes in these pathways (Supplementary Table 5), further strengthening our hypothesis that differences in cuticle and exoskeletal composition may influence variation in hypoxia tolerance. We further propose that the gene *laccase-2* is key in the ability to modulate the composition of the cuticle during hypoxia. This gene is a key mediator of cuticle modifications in invertebrates, where increased expression leads to denser a cuticle (Arakane et al., 2005; Niu et al., 2008; Pan et al., 2009; Ding et al., 2025). It was the 10th most significant differentially expressed gene in Powers and Barreto (2026b), whereby its transcription increased significantly with worsening hypoxia in SD copepods. Our QTL analysis revealed that most SNPs annotated to *lcc2* were intronic (n = 50) or upstream (n = 29), which supports the idea that this gene's influence on tolerance variation is via regulatory divergence among *T. californicus* populations. The location of *lcc2* in an SD-biased QTL is consistent with its strong transcriptional response in SD copepods. Furthermore, its role in melanin pigmentation (Yang et al., 2022) may also impact *T. californicus* management of oxidative stress during hypoxia. Melanin performs protective roles against oxidative stress in invertebrates (Blumenberg, 2017; Wei et al., 2019) and we also detected the melanosome storage gene, *CD63*, in the QTL on chromosome 9. Like *lcc2*, this gene was significantly upregulated during hypoxia (Powers and Barreto, 2026b). Taken together, it is interesting to speculate that *lcc2* may be involved with multiple protective roles in *T. californicus* during hypoxic stress.

In summary, across seven QTL associated with P_{crit} in *T. californicus* hybrids, we found a propensity for variants to occur in putative regulatory regions of genes. Many QTL genes were previously identified as differentially expressed in *T. californicus* from the SD population during a hypoxic event, implying some

genetic variation associated with differences in hypoxia tolerance affects loci that are important to acute physiological responses during hypoxic stress. While SD alleles were the primary contributors to low P_{crit} in our hybrid samples, we observed a strong presence of SH-derived alleles on two QTLs, which is indicative of independent evolutionary trajectories in adaptation to hypoxia. Based on examination of predicted functions of genes with QTLs, we implicated loci that may affect mitochondrial function, sugar metabolism, neurotransmitter flux, and exoskeletal modifications as potential targets for adaptation to hypoxia stress in the face of the absence of the key hypoxia response regulator, *HIF-α*, in the *T. californicus* genome. Future research should aim to test hypotheses concerning the potential roles of exoskeletal composition in *T. californicus* to better understand how invertebrates which use passive oxygen diffusion for respiration can become tolerant to hypoxic stress.

Data availability statement

The datasets presented in this study can be found in online repositories. The names of the repository/repositories and accession number(s) can be found below: https://www.ncbi.nlm.nih.gov/, PRJNA1468271 https://github.com/mjp0044/Hypoxia-Bulk-Segregant-Analysis, GitHub/mjp0044.

Ethics statement

The manuscript presents research on animals that do not require ethical approval for their study.

Author contributions

MP: Investigation, Software, Data curation, Validation, Writing – review & editing, Methodology, Visualization, Supervision, Formal analysis, Writing – original draft. FB: Formal analysis, Methodology, Data curation, Supervision, Project administration, Conceptualization, Software, Funding acquisition, Resources, Writing – review & editing.

Funding

The author(s) declared that financial support was received for this work and/or its publication. This work was supported by a U.S. National Science Foundation research award (award DEB-1556455) to FB.

Acknowledgments

We thank M. Sandoval-Powers and M. Burke for help with genome library preparation, M. Dasenko for help with sequencing, and members of the Burke lab group for feedback on earlier drafts of the manuscript.

Conflict of interest

The author(s) declared that this work was conducted in the absence of any commercial or financial relationships that could be construed as a potential conflict of interest.

Generative AI statement

The author(s) declared that generative AI was not used in the creation of this manuscript.

Any alternative text (alt text) provided alongside figures in this article has been generated by Frontiers with the support of artificial intelligence and reasonable efforts have been made to ensure accuracy, including review by the authors wherever possible. If you identify any issues, please contact us.

Publisher's note

All claims expressed in this article are solely those of the authors and do not necessarily represent those of their affiliated organizations, or those of the publisher, the editors and the reviewers. Any product that may be evaluated in this article, or claim that may be made by its manufacturer, is not guaranteed or endorsed by the publisher.

Supplementary material

The Supplementary Material for this article can be found online at: https://www.frontiersin.org/articles/10.3389/fevo.2026.1900563/full#supplementary-material

References

Alexa, A., and Rahnenfuhrer, J. (2025). Topgo: enrichment analysis for gene ontology. doi: 10.18129/B9.bioc.topGO

Anderson, J. T., Lee, C.-R., Rushworth, C. A., Colautti, R. I., and Mitchell-Olds, T. (2013). Genetic trade-offs and conditional neutrality contribute to local adaptation. *Mol. Ecol.* 22, 699–708. doi: 10.1111/j.1365-294X.2012.05522.x

Arakane, Y., Muthukrishnan, S., Beeman, R. W., Kanost, M. R., and Kramer, K. J. (2005). *Laccase 2* is the phenoloxidase gene required for beetle cuticle tanning. *Proc. Natl. Acad. Sci.* 102, 11337–11342. doi: 10.1073/pnas.0504982102

Barreto, F. S., Watson, E. T., Lima, T. G., Willett, C. S., Edmands, S., Li, W., et al. (2018). Genomic signatures of mitonuclear coevolution across populations of *Tigriopus californicus*. *Nat. Ecol. Evol.* 2, 1250–1257. doi: 10.1038/s41559-018-0588-1

Birk, M. A. (2025). Respirometry: Tools for Conducting and Analyzing Respirometry Experiments. Available online at: http://cran.r-project.org/package=respirometry (Accessed March 16, 2026).

Blumenberg, M. (2017). "Introductory chapter: melanin, a versatile guardian," in *Melanin*. Ed. M. Blumenberg (Rijeka, Croatia: InTech). doi: 10.5772/67599

Burton, R. S., Ellison, C. K., and Harrison, J. S. (2006). The sorry state of F $_2$ hybrids: consequences of rapid mitochondrial DNA evolution in allopatric populations. *Am. Nat.* 168, S14–S24. doi: 10.1086/509046

Castresana, J. (2000). Selection of conserved blocks from multiple alignments for their use in phylogenetic analysis. *Mol. Biol. Evol.* 17, 540–552. doi: 10.1093/oxfordjournals.molbev.a026334

Chen, Q., Ma, E., Behar, K. L., Xu, T., and Haddad, G. G. (2002). Role of trehalose phosphate synthase in anoxia tolerance and development in *Drosophila melanogaster*. *J. Biol. Chem.* 277, 3274–3279. doi: 10.1074/jbc.M109479200

Cingolani, P., Platts, A., Wang, L. L., Coon, M., Nguyen, T., Wang, L., et al. (2012). A program for annotating and predicting the effects of single nucleotide polymorphisms, snpeff. *Fly (Austin).* 6, 80–92. doi: 10.4161/fly.19695

Deconinck, A., and Willett, C. S. (2022). Hypoxia tolerance, but not low pH tolerance, is associated with a latitudinal cline across populations of *Tigriopus californicus*. *PloS One* 17, e0276635. doi: 10.1371/journal.pone.0276635

Ding, Y., Cui, Y., Xie, H., Liang, J., Liu, H., Yuan, F., et al. (2025). Camptothecin weakens the mechanical properties of insect cuticle by inhibiting tanning. *Insect Sci.* 33, 1513–1524. doi: 10.1111/1744-7917.70065

Farrell, A. P., Mueller, C. A., and Seymour, R. S. (2021). Coming up for air. *J. Exp. Biol.* 224(17), jeb243101. doi: 10.1242/jeb.243101

Gavini, C. K., White, C. R., Mansuy-Aubert, V., and Aubert, G. (2022). Loss of C2 domain protein (C2CD5) alters hypothalamic mitochondrial trafficking, structure, and function. *Neuroendocrinology* 112, 324–337. doi: 10.1159/000517273

Gorr, T. A., Wichmann, D., Hu, J., Hermes-Lima, M., Welker, A. F., Terwilliger, N., et al. (2010). Hypoxia tolerance in animals: biology and application. *Physiol. Biochem. Zool.* 83, 733–752. doi: 10.1086/648581

Graham, A. M., and Barreto, F. S. (2019). Loss of the HIF pathway in a widely distributed intertidal crustacean, the copepod *Tigriopus californicus*. *Proc. Natl. Acad. Sci.* 116, 12913–12918. doi: 10.1073/pnas.1819874116

Graham, A. M., and Barreto, F. S. (2020). Independent losses of the hypoxia-inducible factor (HIF) pathway within crustacea. *Mol. Biol. Evol.* 37, 1342–1349. doi: 10.1093/molbev/msaa008

Graham, A. M., and Barreto, F. S. (2023). Myxozoans (Cnidaria) do not retain key oxygen-sensing and homeostasis toolkit genes. *Genome Biol. Evol.* 15(1), evad003. doi: 10.1093/gbe/evad003

Han, K.-L., and Barreto, F. S. (2021). Pervasive mitonuclear coadaptation underlies fast development in interpopulation hybrids of a marine crustacean. *Genome Biol. Evol.* 13 (3), evab004. doi: 10.1093/gbe/evab004

Healy, T. M., Bock, A. K., and Burton, R. S. (2019). Variation in developmental temperature alters adulthood plasticity of thermal tolerance in *Tigriopus californicus*. *J. Exp. Biol.* 222(22), jeb213405. doi: 10.1242/jeb.213405

Healy, T. M., and Burton, R. S. (2023). Genetic incompatibilities in reciprocal hybrids between populations of *Tigriopus californicus* with low to moderate mitochondrial sequence divergence. *Evol. (N. Y).* 77, 2100–2108. doi: 10.1093/evolut/qpad122

Izumi, Y., Yanagihashi, Y., and Furuse, M. (2012). A novel protein complex, mesh-ssk, is required for septate junction formation in *drosophila* midgut. *J. Cell Sci.* 125(20), 4923–4933. doi: 10.1242/jcs.112243

Kaelin, W. G. (2005). Proline hydroxylation and gene expression. *Annu. Rev. Biochem.* 74, 115–128. doi: 10.1146/annurev.biochem.74.082803.133142

Kakinuma, Y., Tsuda, M., Okazaki, K., Akiyama, T., Arikawa, M., Noguchi, T., et al. (2013). Heart-specific overexpression of choline acetyltransferase gene protects murine heart against ischemia through hypoxia-inducible factor-1α–related defense mechanisms. *J. Am. Heart Assoc.* 2(1), e004887. doi: 10.1161/JAHA.112.004887

Kaluz, S., Kaluzová, M., and Stanbridge, E. J. (2008). Regulation of gene expression by hypoxia: integration of the HIF-transduced hypoxic signal at the hypoxia-responsive element. *Clin. Chim. Acta* 395, 6–13. doi: 10.1016/j.cca.2008.05.002

Kenny, T. C., Scharenberg, S., Abu-Remaileh, M., and Birsoy, K. (2025). Cellular and organismal function of choline metabolism. *Nat. Metab.* 7, 35–52. doi: 10.1038/s42255-024-01203-8

Klein, H., Xiao, Y., Conklin, P. A., Govindarajulu, R., Kelly, J. A., Scanlon, M. J., et al. (2018). Bulked-segregant analysis coupled to whole genome sequencing (BSA-Seq) for rapid gene cloning in maize. *G3 Genes|Genomes|Genetics* 8, 3583–3592. doi: 10.1534/g3.118.200499

Li, N., Wang, Z., Zhang, F., Feng, C., Chen, Y., Liu, D., et al. (2024). Threonine dehydrogenase regulates neutrophil homeostasis but not H3K4me3 levels in zebrafish. *FEBS J.* 291, 3367–3383. doi: 10.1111/febs.17138

Li, Z., and Xu, Y. (2022). Bulk segregation analysis in the NGS era: a review of its teenage years. *Plant J.* 109, 1355–1374. doi: 10.1111/tpj.15646

Liepinsh, E., Kuka, J., Vilks, K., Svalbe, B., Stelfa, G., Vilskersts, R., et al. (2021). Low cardiac content of long-chain acylcarnitines in TMLHE knockout mice prevents ischaemia-reperfusion-induced mitochondrial and cardiac damage. *Free Radic. Biol. Med.* 177, 370–380. doi: 10.1016/j.freeradbiomed.2021.10.035

Liu, L., and Manley, J. L. (2024). Modulation of diverse biological processes by CPSF, the master regulator of mRNA 3′ ends. *RNA* 30, 1122–1140. doi: 10.1261/rna.080108.124

Loüytynoja, A., and Goldman, N. (2008). Phylogeny-aware gap placement prevents errors in sequence alignment and evolutionary analysis. *Sci. (1979).* 320, 1632–1635. doi: 10.1126/science.1158395

Lykhmus, O., Izmailov, M., and Skok, M. (2023). Choline derivatives as natural ligands of mitochondrial nicotinic acetylcholine receptors. *Ukr. Biochem. J.* 95, 24–32. doi: 10.15407/ubj95.02.024

Magwene, P. M., Willis, J. H., and Kelly, J. K. (2011). The statistics of bulk segregant analysis using next generation sequencing. *PloS Comput. Biol.* 7, e1002255. doi: 10.1371/journal.pcbi.1002255

Mansfeld, B. N., and Grumet, R. (2018). QTLseqr: an R package for bulk segregant analysis with next-generation sequencing. *Plant Genome* 11, 180006. doi: 10.3835/plantgenome2018.01.0006

Mao, X. R., Moerman-Herzog, A. M., Chen, Y., and Barger, S. W. (2009). Unique aspects of transcriptional regulation in neurons - nuances in NFkappaB and Sp1-related factors. *J. Neuroinflamm.* 6, 16. doi: 10.1186/1742-2094-6-16

Mueller, C. A., and Seymour, R. S. (2011). The regulation index: a new method for assessing the relationship between oxygen consumption and environmental oxygen. *Physiol. Biochem. Zool.* 84, 522–532. doi: 10.1086/661953

Nair, B., Johar, K., Priya, A., and Wong-Riley, M. T. T. (2016). Specificity protein 4 (Sp4) transcriptionally regulates inhibitory GABAergic receptors in neurons. *Biochim. Biophys. Acta (BBA) - Mol. Cell. Res.* 1863, 1–9. doi: 10.1016/j.bbamcr.2015.10.005

Niu, B.-L., Shen, W.-F., Liu, Y., Weng, H.-B., He, L.-H., Mu, J.-J., et al. (2008). Cloning and RNAi-mediated functional characterization of *MaLac2* of the pine sawyer, *Monochamus alternatus*. *Insect Mol. Biol.* 17, 303–312. doi: 10.1111/j.1365-2583.2008.00803.x

Pan, C., Zhou, Y., and Mo, J. (2009). The clone of laccase gene and its potential function in cuticular penetration resistance of Culex pipiens pallens to fenvalerate. *Pestic. Biochem. Physiol.* 93, 105–111. doi: 10.1016/j.pestbp.2008.12.003

Paul, S. M., Ternet, M., Salvaterra, P. M., and Beitel, G. J. (2003). The Na+/K+ ATPase is required for septate junction function and epithelial tube-size control in the *Drosophila* tracheal system. *Development* 130, 4963–4974. doi: 10.1242/dev.00691

Pereira, R. J., Lima, T. G., Pierce-Ward, N. T., Chao, L., and Burton, R. S. (2021). Recovery from hybrid breakdown reveals a complex genetic architecture of mitonuclear incompatibilities. *Mol. Ecol.* 30, 6403–6416. doi: 10.1111/mec.15985

Powers, M., and Barreto, F. (2026a).Data from: transcriptomic adjustment to decreasing oxygen reveals novel functional strategies for extreme hypoxia tolerance in the copepod *Tigriopus californicus Github*. Available online at: https://github.com/mjp0044/Hypoxia-time-series-gene-expression (Accessed May 10, 2026).

Powers, M. J., and Barreto, F. S. (2026b). Transcriptomic adjustment to decreasing oxygen reveals novel functional strategies for extreme hypoxia tolerance in the copepod *Tigriopus californicus*. *Genome Biol. Evol.* 18(2), evag013. doi: 10.1093/gbe/evag013

Powers, M., Schmitz, E., Olvera-Alegria, S., and Barreto, F. (2025). Intertidal copepod *Tigriopus californicus* displays multilevel variation in tolerance to extended bouts of hypoxia. *Mar. Ecol. Prog. Ser.* 757, 53–70. doi: 10.3354/meps14817

R Core Team (2025). R: A Language and Environment for Statistical Computing. Available online at: https://www.R-project.org/ (Accessed June 26, 2026).

Sambrook, J., and Russell, D. W. (2006). Purification of nucleic acids by extraction with phenol:chloroform. *Cold Spring Harb. Protoc.* 2006, pdb.prot4455. doi: 10.1101/pdb.prot4455

Sayols, S. (2023). Rrvgo: a bioconductor package for interpreting lists of gene ontology terms. *MicroPubl. Biol.* 10. doi: 10.17912/micropub.biology.000811

Seibel, B. A., Andres, A., Birk, M. A., Burns, A. L., Shaw, C. T., Timpe, A. W., et al. (2021). Oxygen supply capacity breathes new life into critical oxygen partial pressure (*P* crit). *J. Exp. Biol.* 224(8), jeb242210. doi: 10.1242/jeb.242210

Shen, R., and Messer, P. W. (2022). Predicting the genomic resolution of bulk segregant analysis. *G3 Genes|Genomes|Genetics* 12(3), jkac012. doi: 10.1093/g3journal/jkac012

Song, J., Li, Z., Liu, Z., Guo, Y., and Qiu, L. J. (2017). Next-generation sequencing from bulked-segregant analysis accelerates the simultaneous identification of two qualitative genes in soybean. *Front. Plant Sci.* 8. doi: 10.3389/fpls.2017.00919

Sonobe, T., Kai, Y., Oikawa, S., Akagi, T., Mano, A., Morita, R., et al. (2025). Impaired cardiac non-neuronal acetylcholine synthesis triggers mitochondrial dysfunction with the loss of nicotinic receptor-mediated calcium handling, causing the failing heart. *Clin. Sci.* 139, 1543–1570. doi: 10.1042/CS20257026

Stiburek, L., Fornuskova, D., Wenchich, L., Pejznochova, M., Hansikova, H., and Zeman, J. (2007). Knockdown of human Oxa1l impairs the biogenesis of F1Fo-ATP synthase and NADH:Ubiquinone oxidoreductase. *J. Mol. Biol.* 374, 506–516. doi: 10.1016/j.jmb.2007.09.044

van Niel, G., Charrin, S., Simoes, S., Romao, M., Rochin, L., Saftig, P., et al. (2011). The tetraspanin CD63 regulates ESCRT-independent and -dependent endosomal sorting during melanogenesis. *Dev. Cell* 21, 708–721. doi: 10.1016/j.devcel.2011.08.019

Vaquer-Sunyer, R., and Duarte, C. M. (2008). Thresholds of hypoxia for marine biodiversity. *Proc. Natl. Acad. Sci.* 105, 15452–15457. doi: 10.1073/pnas.0803833105

Walker, J. E., and Dickson, V. K. (2006). The peripheral stalk of the mitochondrial ATP synthase. *Biochim. Biophys. Acta (BBA) - Bioenergetics* 1757, 286–296. doi: 10.1016/j.bbabio.2006.01.001

Wang, Z., Chen, W., Zhang, G., Chi, X., Liu, Z., Wang, H., et al. (2026). CYP6A14 mediates detoxification and antioxidant response in Apis cerana cerana under heavy metal and insecticide stress. *Pestic. Biochem. Physiol.* 219, 107030. doi: 10.1016/j.pestbp.2026.107030

Wang, H.-J., Pochampalli, M., Wang, L.-Y., Zou, J. X., Li, P.-S., Hsu, S.-C., et al. (2019). KDM8/JMJD5 as a dual coactivator of AR and PKM2 integrates AR/EZH2 network and tumor metabolism in CRPC. *Oncogene* 38, 17–32. doi: 10.1038/s41388-018-0414-x

Wei, L., Jiang, Q., Cai, Z., Yu, W., He, C., Guo, W., et al. (2019). Immune-related molecular and physiological differences between black-shelled and white-shelled Pacific oysters *Crassostrea gigas*. *Fish Shellfish Immunol.* 92, 64–71. doi: 10.1016/j.fsi.2019.05.056

Wu, V. M., and Beitel, G. J. (2004). A junctional problem of apical proportions: epithelial tube-size control by septate junctions in the *Drosophila* tracheal system. *Curr. Opin. Cell Biol.* 16, 493–499. doi: 10.1016/j.ceb.2004.07.008

Yang, Z. (2007). PAML 4: Phylogenetic analysis by maximum likelihood. *Mol. Biol. Evol.* 24, 1586–1591. doi: 10.1093/molbev/msm088

Yang, Q., Liu, J.-Y., Liu, S.-M., Song, W.-J., Tian, Y.-P., and Li, M.-Y. (2026). Deubiquitinase USP5 promotes acute myeloid leukemia through C2CD5 stabilization and PI3K/AKT/mTOR/HIF-1α-driven glycolysis. *Biochem. Pharmacol.* 244, 117591. doi: 10.1016/j.bcp.2025.117591

Yang, Z., and Nielsen, R. (2000). Estimating synonymous and nonsynonymous substitution rates under realistic evolutionary models. *Mol. Biol. Evol.* 17, 32–43. doi: 10.1093/oxfordjournals.molbev.a026236

Yang, C.-H., Zhang, Q., Zhu, W.-Q., Shi, Y., Cao, H.-H., Guo, L., et al. (2022). Involvement of Laccase2 in cuticle sclerotization of the whitefly, *Bemisia tabaci* Middle East–Asia Minor 1. *Insects* 13, 471. doi: 10.3390/insects13050471

Yoshida, S., Tsutsumi, S., Muhlebach, G., Sourbier, C., Lee, M.-J., Lee, S., et al. (2013). Molecular chaperone TRAP1 regulates a metabolic switch between mitochondrial respiration and aerobic glycolysis. *Proc. Natl. Acad. Sci.* 110(17), E1604–E1612. doi: 10.1073/pnas.1220659110

Zhang, X., Guan, L., Zhang, Y., Zhong, F., Xie, Y., Zhang, Y., et al. (2025). *TcCYP4C1* in combination with trehalose to cope with high-CO_2 stress in *Tribolium castaneum* (Coleoptera). *Insect Mol. Biol.* 34, 729–742. doi: 10.1111/imb.12997

Zhang, B., Qi, F., Hu, G., Yang, Y., Zhang, L., Meng, J., et al. (2021). BSA-seq-based identification of a major additive plant height QTL with an effect equivalent to that of Semi-dwarf 1 in a large rice F2 population. *Crop J.* 9, 1428–1437. doi: 10.1016/j.cj.2020.11.011

Zheng, Y., Xu, F., Li, Q., Wang, G., Liu, N., Gong, Y., et al. (2018). QTL mapping combined with bulked segregant analysis identify SNP markers linked to leaf shape traits in *Pisum sativum* using SLAF sequencing. *Front. Genet.* 9. doi: 10.3389/fgene.2018.00615